CHEMISTRY OF MATERIALS
Article

Chem. Mater. **2009,** *21,* 4851–4858 4851
DOI:10.1021/cm9023327

Synthesis of Ordered Layers of Monodisperse $CoFe_2O_4$ Nanoparticles for Catalyzed Growth of Carbon Nanotubes on Silicon Substrate

Claudia Altavilla,*,† Maria Sarno,†,‡ and Paolo Ciambelli†,‡

†*Department of Chemical and Food Engineering, University of Salerno, via Ponte Don Melillo, 84084 Fisciano (SA), Italy, and* ‡*Centre NANO_MATES, University of Salerno, 84081 Baronissi (SA), Italy*

Received July 29, 2009. Revised Manuscript Received September 14, 2009

Simple and inexpensive formation of extended and ordered mono- or multilayers of highly monodispersed $CoFe_2O_4$ nanoparticles, covered by oleic acid coating, was obtained by the spin-coating method on silicon substrate. Two concentrations of nanoparticles dispersions were employed. The oleic-capped nanoparticles were used as catalysts for the growth of carbon nanotubes by ethylene CCVD. A close correlation of nanotube diameter with nanoparticle size has been verified. Moreover, density and length of nanotubes can be controlled by nanoparticle concentration.

1. Introduction

Metal and metal-oxide nanoparticles have been attracting intensive interest thanks to the nanoscopic size of the inorganic core, which generates new properties unique to quantum-confined structures.

In this wide variety of materials, the family of ferrites with general formula MFe_2O_4 (M = Fe,Co,Ni, etc.) is intensively studied for various applications because of chemical stability biocompatibility and magnetic properties of its members.[1−4]

In particular, $CoFe_2O_4$ nanoparticles (NPs) with controlled shape and size are appealing for high-density recording applications.[5−8] Moreover, ferrite nanoparticles, when covered by an appropriate organic coating,[9] have also attracted great interest in the biomedical field, especially in magnetic targeted drug delivery and in magnetic fluid hyperthermia, because of their larger magnetic anisotropy and magnetic moments than those for iron oxides.[10,11]

Thanks to the high surface/volume ratio, another application of ferrite nanoparticles is the catalyzed growth of monodimensional nanostructures by chemical vapor deposition (CCVD) technique. Recently, monodispersed Fe_3O_4 nanoparticles have been investigated as catalyst for CCVD synthesis of boron nanowires[12] and carbon nanotubes.[13,14]

A crucial aspect for the most applications cited before is the ability to control the assembly of nanoparticles to realize films, arrays, patterns, networks and circuits for the fabrication of novel nanodevices. While traditional approaches based on "top-down" techniques (lithography, ion sputtering depositions, laser ablation, etc.) require very expensive equipment, wet coating methods based on "bottom-up" chemical strategies may offer many advantages such as experimental facility and potential low-cost fabrication. High productivity of highly ordered nanostructures on a substrate is the present target that may have revolutionary effects for science and technology.[15]

In this work we focus the attention on the synthesis of high monodispersed oleic acid-capped $CoFe_2O_4$ nanoparticles and their simple and inexpensive assembly on silicon substrate by the spin-coating method. The formation of extended and ordered mono- or multilayers of $CoFe_2O_4$ nanoparticles, exploitable for many applications, is here used to examine their catalytic properties for the growth of carbon nanotubes. In previous work, we obtained high selectivity and yield in

*Corresponding author. E-mail: caltavilla@unisa.it.

(1) Altavilla, C.; Ciliberto, E.; Gatteschi, D.; Sangregorio, C. *Adv. Mater*. **2005**, *17*, 1084.
(2) Xu, Z. P.; Zeng, Q. H.; Lu, G. Q.; Yu, A. B. *Chem. Eng. Sci*. **2006**, *6*, 1027.
(3) Maier-Hauff, K.; Rothe, R.; Scholz, R.; Gneveckow, U.; Wust, P.; Thiesen, B.; Feussner, A.; von Deimling, A.; Waldoefner, N.; Felix, R.; Jordan, A. *J. Neurooncol*. **2007**, *81*, 53.
(4) Gomes, J. A.; Sousa, M. H.; Tourinho, F. A.; Aquino, R.; da Silva, G. J.; Depeyrot, J.; Dubois, E.; Perzynski, R. *J. Phys. Chem. C* **2008**, *112*, 6220.
(5) de Vicente, J.; Delgado, A. V.; Plaza, R. C.; Duràn, J. D. G; Gonzàlez-Caballero, F. *Langmuir* **2000**, *16*, 7954.
(6) Liu, Z.; Li, X.; Leng, Y. *J. Nanomater*. **2008**, *2008*, No. doi:10.1155/2008/921654.
(7) Altavilla, C.; Ciliberto, E.; Aiello, A.; Sangregorio, C.; Gatteschi, D. *Chem. Mater*. **2007**, *19*, 5980.
(8) Bhattacharyya, S.; Salvetat, J.-P.; Fleurier, R.; Husmann, A.; Cacciaguerra, T.; Saboungia, L. *Chem. Commun*. **2005**, 4818.
(9) Colognato, R.; Bonelli, A.; Bonacchi, D.; Baldi, G.; Migliore, L. *Nanotoxicology* **2007**, *1*, 301.
(10) Baldi, G.; Bonacchi, D.; Comes Franchini, M.; Gentili, D.; Lorenzi, G.; Ricci, A.; Ravagli, C. *Langmuir* **2007**, *23*, 4026.
(11) Kückelhaus, S.; Reis, S. C.; Carneiro, M. F.; Tedesco, A. C.; Oliveira, D. M.; Lima, E. C. D.; Morais, P. C.; Azevedo, R. B. Z.; Lacava, G. M. *J.Magn. Magn. Mater*. **2004**, *2402*, 272.
(12) Xu, Z.; Shen, C.; Hou, Y.; Gao, H.; Sun, S. *Chem. Mater*. **2009**, *21*, 1778.
(13) Dupuis, A.-C. *Prog. Mater. Sci*. **2005**, *50*, 929.
(14) Debmalya, R.; Kanik, R. *Synth. Met*. **2009**, *159*, 343.
(15) Altavilla, C. Innovative Methods in Nanoparticles Assembly. In *Advanced Materials: Research Trends*; Levan, A., Ed.; Nova Science Publishers: New York, 2007; Chapter 4, pp. 217−-236.

Published on Web 10/05/2009

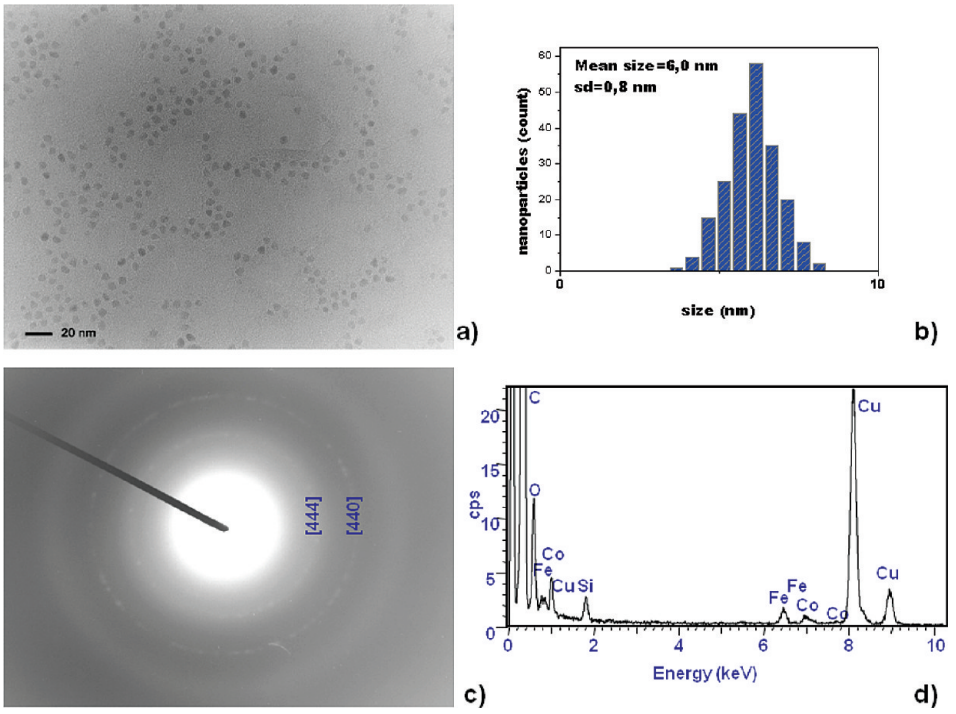

Figure 1. Characteristics of $CoFe_2O_4$ nanoparticles: (a) TEM image; (b) size distribution; (c) electron diffraction pattern; (d) EDX spectrum.

synthesizing carbon nanotubes on supported cobalt and iron catalyst.[16,17]

NPs synthesis and CCVD growth of carbon nanotubes are described and the possibility to control density, length, and assembly of nanotubes on silicon wafer is discussed.

2. Experimental section

2.1. Materials. Ethanol, toluene, sulphuric acid (98%), and hydrogen peroxide (30%) were used as received. Phenyl ether (99%), 1,2-hexadecanediol (97%), oleic acid (90%), oleylamine (>70%), cobalt(II) acetylacetonate, and iron(III) acetylacetonate were purchased from Aldrich. Water of Milli Q quality was obtained from Millipore water purification equipment (Bedford, MA). Monocrystalline oriented silicon wafers (100) were kindly provided by ST Microelectronics of Catania (Italy).

2.2. Synthesis of $CoFe_2O_4$ Nanoparticles. NPs were prepared by thermal decomposition of iron and cobalt acetylacetonates in organic solvent using a mixture of surfactant agents. $Fe(acac)_3$ (2 mmol), $Co(acac)_2$ (1 mmol), 1,2-hexadecanediol (10 mmol), oleic acid (6 mmol), oleylamine (6 mmol), and phenyl ether (20 mL) were mixed and magnetically stirred under a nitrogen flow. The mixture was heated to reflux (265 °C) for 60 min. The black-brown mixture was cooled to room temperature by removing the heat source. The product was washed with ethanol, centrifuged, and finally dissolved in 40 mL of toluene, forming a dispersion stable over a long period of time.[18,19]

2.3. Preparation of Silicon Substrate. Oriented silicon wafer (100) was cut into 1×1 cm^2 pieces, that were sonically cleaned in toluene, acetone and Milli Q water for periods of 15 min. After cleaning, the substrates were soaked in piranha solution [H_2SO_4 (98%)/H_2O_2 (30%) 1:3 by volume], washed with Milli Q water, and dried under a nitrogen flow.

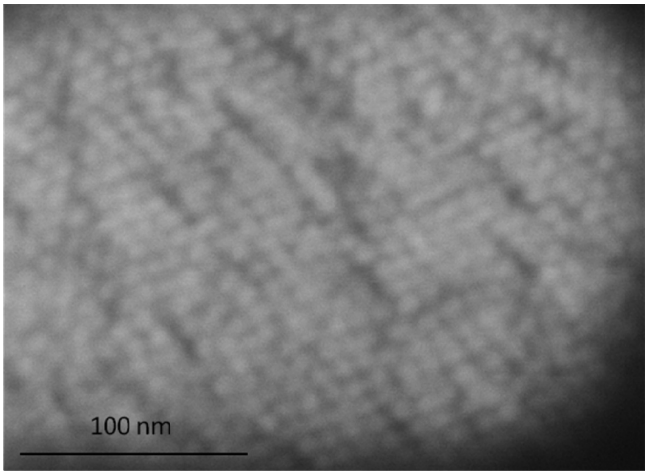

Figure 2. FE-SEM image of hexagonally packed superlattice of $CoFe_2O_4$ nanoparticles obtained by spin-coating deposition on silicon substrate.

2.4. Formation of Ordered Layer of Nanoparticles on a Silicon Substrate. The spin coating technique was used to spread the synthesized nanoparticles on silicon wafer. The rotational speed was set at 4000 rpm and the time of spinning was 10 min. We used a toluene dispersion of nanoparticles either as-obtained after synthesis or after dilution in volume to a 1:8 ratio.

Two silicon substrates were used for CCVD synthesis of carbon nanotubes: HDNP (silicon covered by high-density nanoparticles film) was prepared by spin coating of the concentrated NPs dispersion on the silicon wafer, LDNP (silicon covered by low-density nanoparticles film) was obtained by spin-coating of diluted NP dispersion in the same conditions as for HDNP.

2.5. CCVD Growth of Carbon Nanotubes (CNT). HDNP and LDNP substrates were mounted into a vertical quartz tube

(16) Ciambelli, P.; Sannino, D.; Sarno, M.; Fonseca, A; Nagy, J. B. *Carbon* **2005**, *43*, 631.
(17) Ciambelli, P.; Sannino, D.; Sarno, M.; Leone, C.; Lafont, U. *Diamond Relat. Mater.* **2007**, *16*, 1144.
(18) Sun, S. H.; Zeng, H.; Robinson, D. B.; Raoux, S.; Rice, P. M.; Wang, S. X.; Li, G. X. *J. Am. Chem. Soc.* **2004**, *126*, 273.
(19) Sun, S. H.; Zeng, H. *J. Am. Chem. Soc.* **2002**, *124*, 8204.

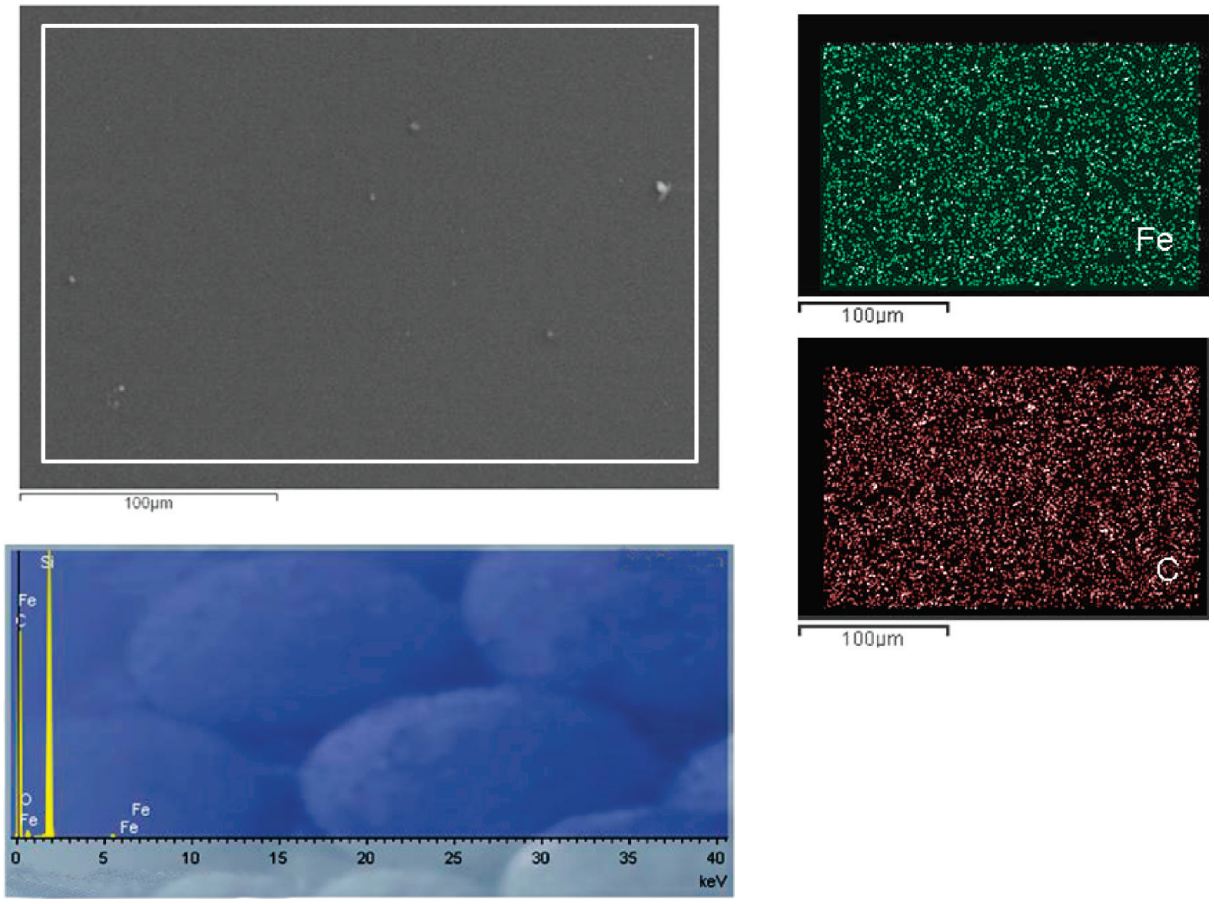

Figure 3. From left to right clockwise: (i) low-resolution FESEM image of silicon substrate covered by diluted dispersion of cobalt ferrite nanoparticles; (ii) EDX map, and (iii) relevant spectrum of Fe and C (a thin film of chromium was evaporated on the sample to made it conductive during acquisition of EDX maps).

reactor and introduced in a preheated furnace at 700 °C for 10 min under a N_2 atmosphere. Pure N_2 flow was replaced by a gas mixture of C_2H_4 (99.998 pure) with the flow rate of 8 (stp) cm^3/min in N_2 (99.999 pure) (72 (stp) cm^3/min) and maintained at 700 °C for 60 min. The reactor was then cooled to room temperature under a N_2 flow and the substrates were recovered. They were named, respectively, CNTHDNP and CNTLDNP.

2.6. Characterization Techniques. TEM micrographs of cobalt ferrite nanoparticles were obtained using a JEOL JEM 2010 electron microscope operating at 200 kV.

Field emission scanning electron microscopy (FESEM) images were collected with a FESEM LEO 1550 VP microscope. Energy-dispersive X-ray analyses were acquired with a FESEM LEO 1525 microscope equipped with a EDX detector. To obtain the EDX maps that require long acquisition times, we covered the samples with chromium film to made them conductive.

The thermal decomposition behavior of nanoparticles organic coating was investigated with a thermo-analyzer (Q600, TA Instruments) online connected to a quadrupole mass detector (Quadstar 422, Pfeiffer Vacuum). The measurement was carried out in nitrogen flow, under the same temperature-programmed heating (from room temperature to 700 °C) as before the CVD synthesis.

Raman spectra were obtained with a micro Raman spectrometer Renishaw inVia (514 nm excitation wavelength).

3. Results and Discussion

3.1. Nanoparticle Characterization. The morphological and structural characteristics of the cobalt ferrite particles were determined by transmission electron microscopy (TEM) analysis. The images revealed the formation of nanoparticles with highly uniform size that, once deposited over a copper grid, tend to self-organize in a regular hexagonal layer (Figure 1a). The particle size distribution, obtained from statistic analysis of over 200 nanoparticles, is shown in Figure 1b. The average diameter of inorganic core is $d = 6.0$ nm with $\sigma = \pm 0.8$. The corresponding electron diffraction pattern (Figure 1c) and the EDX spectrum (Figure 1d) confirm the ferrite nature of nanocrystals.[17]

The samples obtained by spin coating the organic dispersion of nanoparticles onto Si wafer, following the procedure described in the Experimental Section, were examined by FESEM. We found that the coating procedure allowed to form an extended ordered layer of $CoFe_2O_4$ nanoparticles on the silicon wafer surface. A typical FESEM image (Figure 2) clearly shows a densely packed film of nanoparticles formed after spin coating deposition. The hexagonally packed superlattice, stable even after solvent evaporation, was obtained thanks to the high monodispersion of nanoparticles and to the hydrophobic interactions of organic chains that cover the surface of NPs.

To investigate the effect of the concentration of dispersion on the characteristics of the nanoparticles layer, we analyzed LDNP and HDNP samples by EDX.

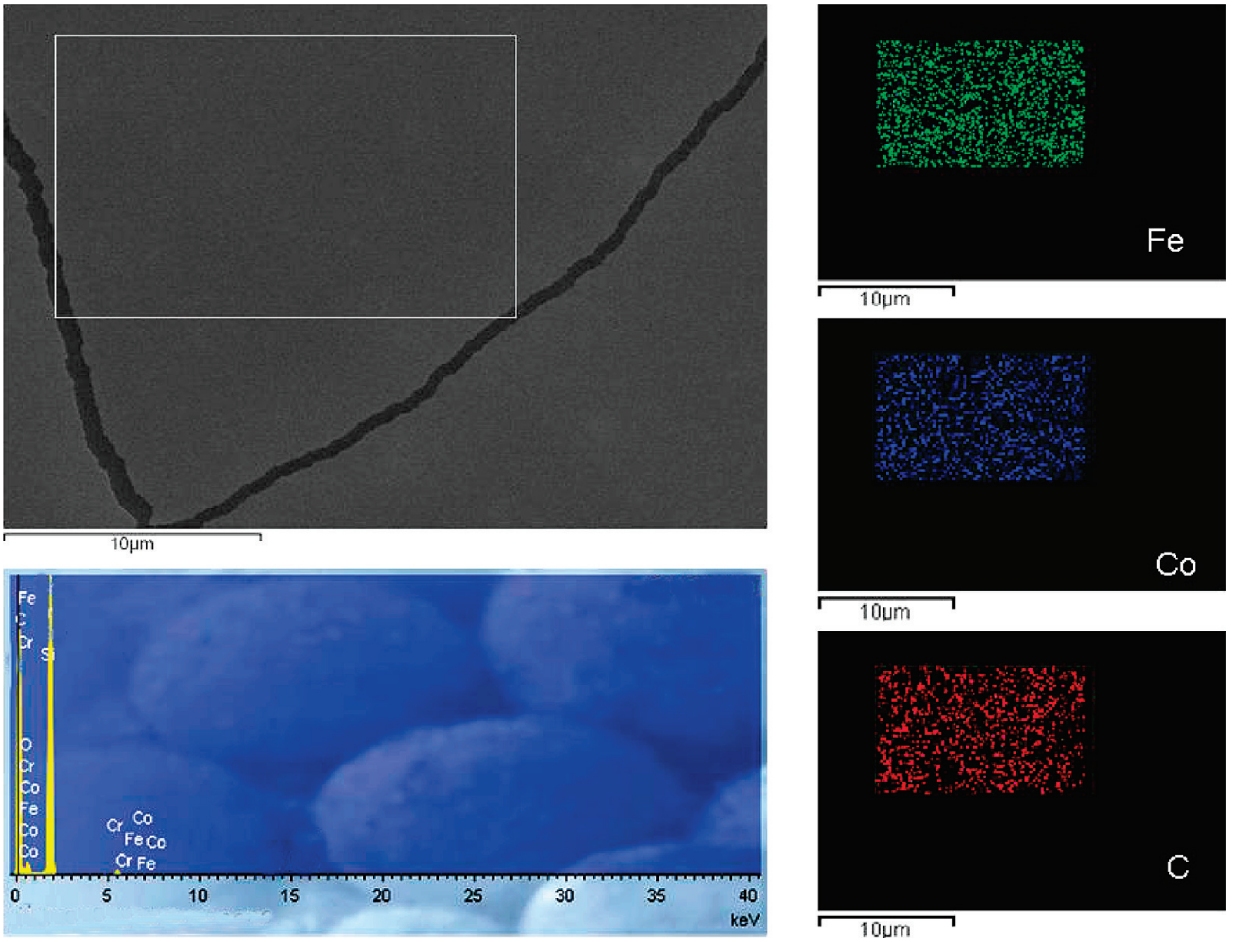

Figure 4. From left to right clockwise: (i) low-resolution FESEM image of silicon substrate covered by concentrated dispersion of cobalt ferrite nanoparticles, (ii) EDX map, and (iii) relevant spectrum of Fe, Co, and C.

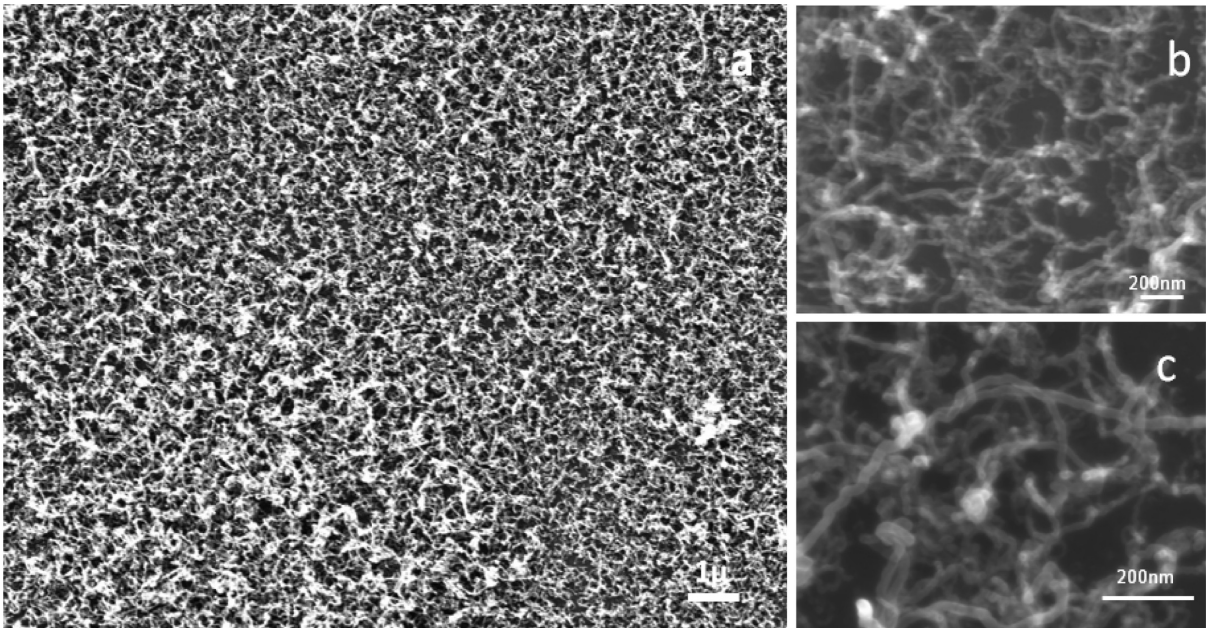

Figure 5. (a) Low-resolution image of synthesized carbon nanotubes on LDNP by catalytic decomposition of C_2H_4 at 700 °C for 60 min; (b, c) higher-magnification images of details.

Figure 3 shows typical results obtained with the sample LDNP. The low concentration of NPs on the substrate permitted to collect only X-ray dispersive energy signals of Fe (green) and C (red) with their corresponding EDX chemical maps. It was not possible to collect the chemical map of Co, because cobalt, present in ferrite at a 0.5 atomic

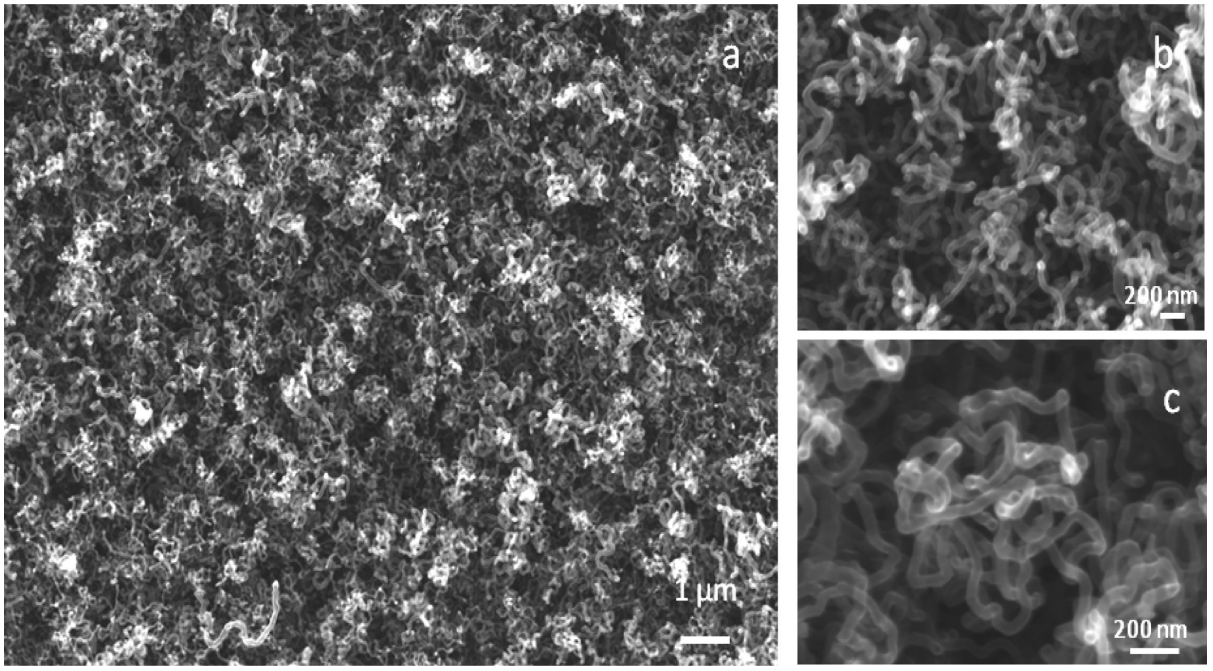

Figure 6. (a) Low-resolution FESEM image of synthesized carbon nanotubes on HDNP by catalytic decomposition of C_2H_4 at 700 °C for 60 min; (b, c) images of details at higher magnifications.

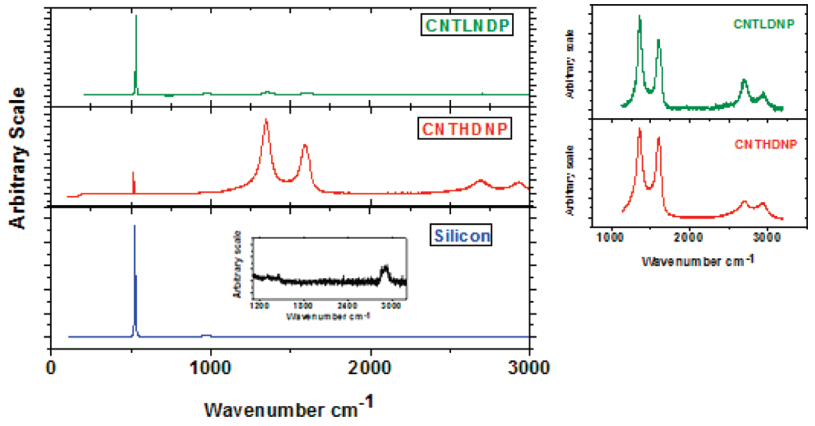

Figure 7. Wide Raman spectra of CNTLDNP, CNTHDNP, and untreated silicon substrate up to 3000 cm^{-1} (left side); Raman spectra of CNTLDNP and CNTHDNP in the range 1000−3000 cm^{-1} (right side).

ratio with respect to iron, has a concentration value under the detection limit of the instrument. The EDX signal from carbon is due to the organic coating of ferrite particles. The chemical maps of Fe and C suggest that a homogeneous distribution of NPs on the substrate was obtained using spin coating to spread nanoparticles on silicon.

EDX characterization of HDNP (Figure 4) shows that in this case, the higher concentration of the nanoparticle film allowed us to collect chemical maps of Fe, Co and C, from which it is clearly evidenced that densely packed film of nanoparticles formed on the silicon substrate. Moreover, the measured atomic concentration ratio between Fe and Co (2:1) confirmed the stoichiometry of ferrite for the nanoparticles.

3.2. Synthesis of Carbon Nanotubes. Both samples LDNP and HDNP were tested for CCVD of carbon nanotubes.

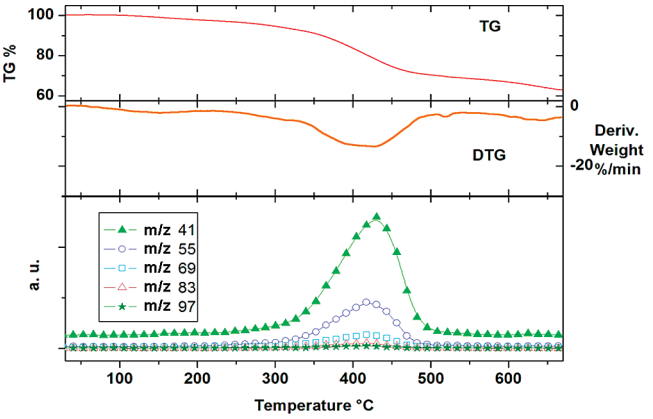

Figure 8. TG, DTG curves, and MS evaluation of oleic acid-capped cobalt ferrite nanoparticles.

A low-resolution FESEM image of the sample CNT-LDNP is reported in Figure 5a, showing a disordered film of

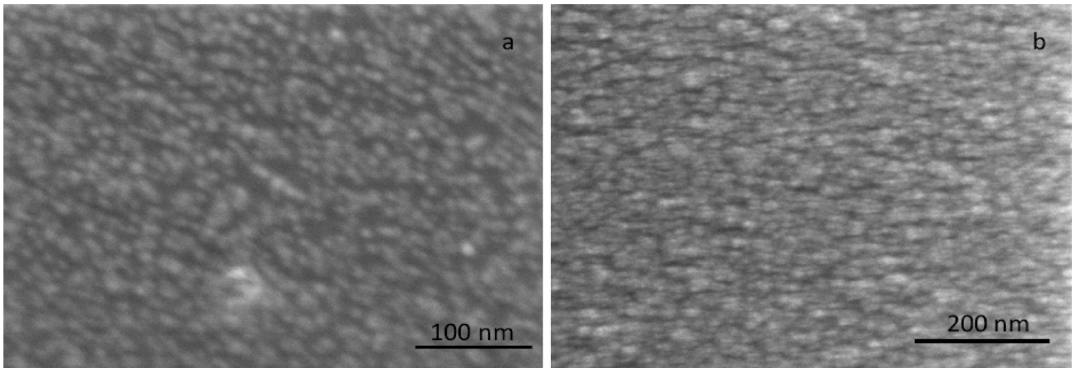

Figure 9. Effect of annealing pretreatment on the morphology of the catalytic films. (a) FE-SEM image of LDNP after pretreatment at 700 °C; (b) FE-SEM image of HDNP after pretreatment at 700 °C.

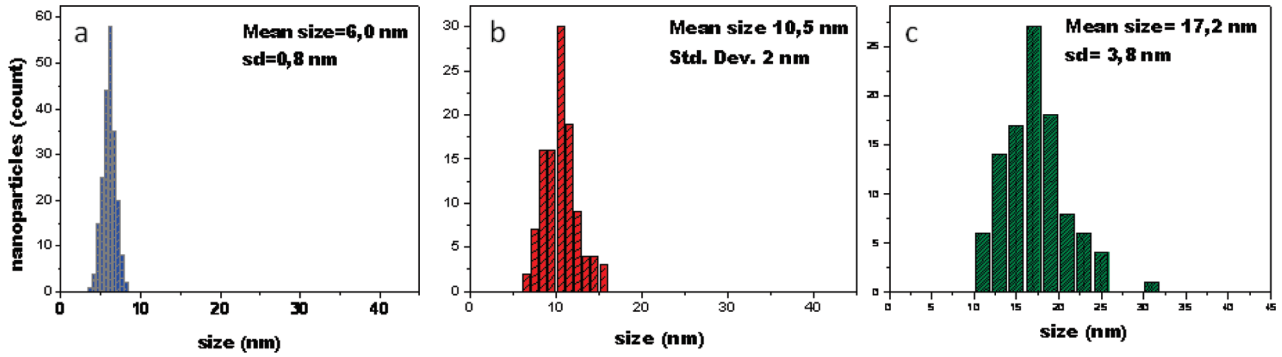

Figure 10. (a) Size distribution histogram evaluated by TEM of inorganic core of cobalt ferrite nanoparticles before annealing; b) size distribution histogram evaluated by FESEM nanoparticles on LDNP after annealing at 700 °C; (c) size distribution histogram evaluated by FESEM nanoparticles on HDNP after annealing at 700 °C.

carbon nanotubes covering uniformly a large substrate area. The images collected at higher magnification (images b and c in Figure 5) allowed us to evaluate the organization of CNTs on silicon substrate as low-density tangles of transparent carbon nanotubes whose diameters are around 20 nm and lengths are in the range of hundreds of nanometers.

In Figure 6a, a low-resolution FESEM image of the sample CNTHDNP is reported, showing a thick carpet of carbon nanotubes on the silicon substrate. TEM images obtained at higher magnification (see figure 6b and 6c) show tangles of transparent CNTs on silicon substrate with diameters around 40 nm and length in the range of micrometers.

Raman spectroscopy was used to obtain some indication on the quality of MWNTs. Figure 7 shows typical D and G bands that indicate the presence of crystalline graphite carbon and defects, respectively, for both CNTHDNP and CNTLDNP. D and G bands (see the spectra in the range 1000−3200 cm^{-1}) are centered at 1355 and 1606 cm^{-1}, respectively. The values of the I_D/I_G intensity ratio, which is a measure of disorder, increase from 1.15 for CNTHDNP to 1.38 for CNTLDNP, indicating a higher order for the CNTs synthesized at a higher nanoparticle concentration, partially because of the lower impact of finite size of crystalline domains of longer carbon nanotubes. The spectra exhibit also the second-order 2D band that is indicative of an high crystalline quality and absence of impurities.[17,20]

Peaks of silicon are clearly visible in the spectrum of CNTHDNP (see in the figure the spectrum of not treated silicon). They are better resolved in the case of CNTLDNP, which has a lower nanotube content.

All the results suggest that density, length, diameter, and grade of order of CNTs are influenced by the density of ferrite nanoparticles film on silicon wafer.

However, a proper discussion of the above conclusions must take into account how the presence of the organic layer and the heating of catalyzed silicon samples to the conditions required for the growth of carbon nanotubes could have affected the obtained results.

In fact, in the first case, it must be considered that, together with ethylene, the organic layer is also a potential carbon source for carbon nanotubes growing. Therefore, with the aim of determining the thermal behavior of the oleic acid coating and, consequently, evaluating a possible contribution from it to the total carbon deposited during the CVD process, a TG-DTG analysis of Co_2FeO_4 nanoparticles was performed under N_2 atmosphere and in the same conditions as for the CVD pretreatment. The ion currents of the most 5 intense mass fragments (m/z = 41, 55, 69, 83, 97) of oleic acid were acquired by the mass detector interfaced to the TG analyzer.

The results reported in Figure 8 show a wide mass loss from 310 to 490 °C: the ion currents of fragments detected in the same temperature range suggest that the loss was due to oleic acid decomposition. Therefore, this result suggests that during the CVD process no contribution to

(20) Sveningsson, M.; Morjan, R.-E.; Nerushev, O. A.; Sato, Y.; Bäckström, J.; Campbell, E. E. B.; Rohmund, F. *Appl. Phys. A: Mater. Sci. Process.* **2001**, *73*, 409.

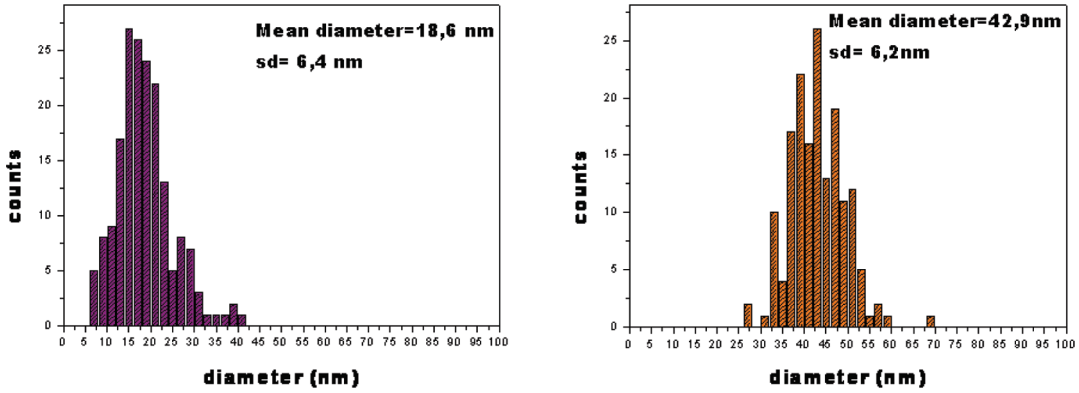

Figure 11. External diameter distribution of nanotubes CNTLDNP(on the right in purple) and CNTHDNP (on the right in orange).

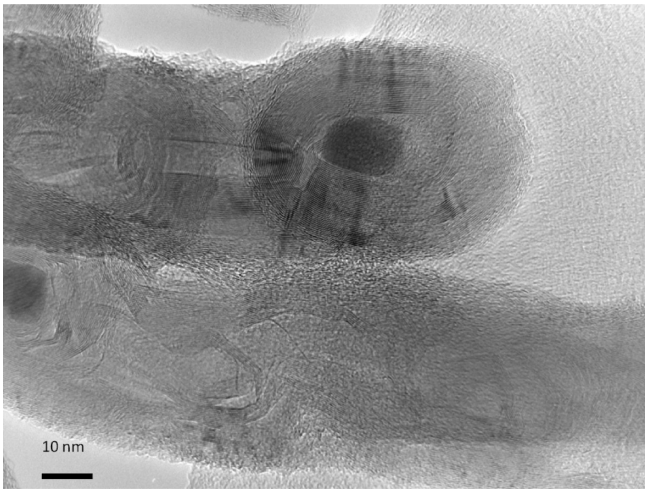

Figure 12. TEM image of a catalytic nanoparticle enclosed in the nanotube.

the total deposited carbon is attributable to the organic coating of cobalt ferrite particles, because of it was completely decomposed to gas products during the pretreatment, before reaching the temperature at which the catalyst is active for CNT growing.

With respect to the second point of discussion, it is expected that high temperature generally induces coalescence between the closest particles. Therefore, the effect of annealing pretreatment on the morphology of the catalytic film was investigated by FESEM.

The image of LDNP after pretreatment at 700 °C (Figure 9a) shows that the concentration of cobalt ferrite nanoparticles dispersion was not sufficient to completely cover the silicon support with a densely packed nanoparticles monolayer. Moreover, the evaluation of the size distribution of inorganic clusters upon pretreatment indicates that a moderate coalescence phenomenon was occurred. In fact, the average size of nanoparticles (inorganic core) shifted from 6.0 nm ± 0.8 nm (as evaluated by TEM, see blue histogram in Figure 10a) before annealing, to 10.5 nm ± 2 nm after the treatment (see red histogram in Figure 10b).

For the sample HDNP the same characterization was carried out before and after CCVD synthesis of carbon nanotubes. In particular, the typical FESEM image of HDNP after pretreatment at 700 °C, reported in Figure 9b, shows that this dispersion, eight times more concentrated than LDNP, allowed a densely packed nanoparticle film to form, completely covering the substrate. Even in this case, the annealing pretreatment caused a coalescence, with a shift in nanoparticle average size from 6.0 nm ± 0.8 nm (as evaluated by TEM) to 17.2 nm ± 3.8 nm (see green histogram in Figure 10c).

Table 1. Values of Nanoparticle Size and Nanotubes Diameters

	NPs size (nm) after annealing at 700 °C	internal diameter of CNT (nm)	external diameter of CNT (nm)
CNTLDNP	10.5 ± 2	12.3 ± 3.6	18.6 ± 6.4
CNTHDNP	17.2 ± 3.8	19.7 ± 4.2	42.9 ± 6.2

Concerning the dimension of CNTs obtained with the two silicon samples, the diameter size distribution of nanotubes grown on silicon-deposited LDNP (see purple histogram in Figure 11) shows an average value of 18.6 nm with a standard deviation of ± 6.4 nm. In the case of HDNP, from the external diameter distribution of nanotubes (see orange histogram in Figure 11), an average size of 42.9 nm with a standard deviation of ±6.2 nm was evaluated.

The TEM image reported in Figure 12 shows a catalytic nanoparticle enclosed in the nanotube.

The estimation of nanotube inner diameter for both samples gives values consistent with the nanoparticles dimension after annealing: average value of 12.3 nm ± 3.6 nm for inner diameter of CNTLDNP and average value of 19.7 nm ± 4.2 nm for inner diameter of CNTHDNP. They are in very good agreement with those relevant to the annealed nanoparticles from which the nanotubes were grown (Table 1). Therefore, the size of cobalt ferrite nanoparticles determines the inner diameter of the grown carbon nanotube.

4. Conclusions

We have found that the presence of oleic acid and of oleylammine in the reaction mixture has assured the formation of hexagonally packed superlattices of monodispersed cobalt ferrites nanoparticles. The spin-coating technique has permitted us to control the density of the nanoparticle film by varying the concentration of

nanoparticle dispersion and has assured an homogeneous distribution of nanoparticles on a large substrate area.

The $CoFe_2O_4$ nanoparticles on silicon catalyzed the growth of carbon nanotubes. The morphology of MWNT tangles formed seems to be strongly dependent on thickness and density of catalytic film.

A more concentrated solution gives rise to the formation, at the end of the pretreatment, of larger particles, which leads to the formation of MWNTs with larger diameters. A close correlation of nanotube diameter with nanoparticle size has been verified. Additionally, CNT density and length can be also controlled by NPs concentration.

Further work is in progress to evaluate the catalytic properties of ferrite nanoparticles with different size to grow CNT on patterned silicon substrate.

Acknowledgment. The authors acknowledge Prof. Enrico Ciliberto for FESEM characterization of CNTs and of catalytic films and Mr. Claudio Uliana and Miss Laura Negretti for TEM characterization of nanoparticles and carbon nanotubes.